

RNASEH1-AS1 induced by H3K27ac stabilizes ANXA2 mRNA to promote the progression of colorectal cancer through recruiting BUD13

Shengwei ZHUANG*, Weihong LU*, Lianjun SHEN*, Zhekun HUANG, Xiuping ZHANG, Yong ZHANG*

Zhongshan Hospital (Xiamen), Fudan University; Xiamen Clinical Research Center for Cancer Therapy, Xiamen, Fujian, China

*Correspondence: zhangyong123678@163.com

*Contributed equally to this work.

Received June 12, 2023 / Accepted September 20, 2023

Colorectal cancer (CRC) is a malignant tumor with high morbidity and mortality. It is well-accepted that dysregulated lncRNAs are closely related to the development of CRC. In this study, the function and mechanism of RNASEH1-AS1 in CRC were investigated. RT-qPCR and western blot detected the expression of targeted genes in tissues and cells. CCK-8, clone formation, wound healing assay, and Transwell were applied to evaluate CRC cell malignant behaviors. ChIP, RIP, and RNA pull-down validated interactions among RNASEH1-AS1, H3K27ac, CBP, BUD13, and ANXA2. Nucleoplasmic separation and FISH assay determined the location of RNASEH1-AS1 in CRC cells. IHC assay was used to detect Ki-67 expression in tumor tissues from mice. RNASEH1-AS1 was highly expressed in CRC tumor tissues and cells. RNASEH1-AS1 silencing effectively suppressed the viability, proliferation, migration, and invasion of CRC cells. In addition, CBP-mediated H3K27ac increased RNASEH1-AS1 expression in CRC cells and RNASEH1-AS1 could elevate ANXA2 expression through recruiting BUD13. Furthermore, RNASEH1-AS1 silencing inhibited malignant phenotypes of CRC cells and tumor growth in mice through decreasing ANXA2 expression and inactivating the Wnt/ β -catenin pathway. Our results revealed that RNASEH1-AS1 induced by CBP-mediated H3K27ac activated Wnt/ β -catenin pathway to promote CRC progression through recruiting BUD13 to stabilize ANXA2 mRNA, which provides substantial evidence of RNASEH1-AS1 in CRC. Targeting RNASEH1-AS1 might alleviate CRC progression.

Key words: colorectal cancer; H3K27ac; RNASEH1-AS1; BUD13; ANXA2

Colorectal cancer (CRC) is a common gastrointestinal malignant tumor. According to an authoritative statistic, CRC accounts for 9.8 percent of all new cancer cases and 9.2% of all cancer deaths in 2020 [1]. CRC therapies mainly include surgery, chemoradiotherapy, which have achieved favorable prognosis [2]. However, due to the majority of CRC patients being diagnosed with advanced CRC, invasion and distant metastasis pose serious challenges [3]. At present, the molecular pathogenesis of CRC has not been explicitly illustrated, which needs more studies.

Long noncoding RNAs (lncRNAs), belonging to non-coding RNA, are widely found in eukaryotes and play an indispensable role [4]. Massive evidence has demonstrated that lncRNAs such as lncRNA TM4SF19-AS1, lncRNA DLGAP1-AS2 were implicated in tumor progression including CRC [5, 6]. lncRNA RNASEH1-AS1 was documented to be upregulated in non-small cell lung cancer (NSCLC) and its silencing effectively suppressed NSCLC

progression [7]. Currently, RNASEH1-AS1 has been poorly reported in diseases, so does it affect the progression of CRC? starBase revealed that RNASEH1-AS1 had abnormally higher expression in CRC, indicating the potential functions of RNASEH1-AS1 in CRC, which inspired us to explore its functions and underlying mechanism.

It has been reported that lncRNAs affect diseases by interacting with RNA-binding protein (RBP) to regulate the expression of targeted genes [8]. For instance, lncRNA TRPM2-AS interacted with TAF15 (an RBP) to promote the mRNA stability of TRPM2, thereby accelerating CRC cell proliferation [9]. It was documented that BUD13 homolog (BUD13) played biological roles as an RBP for circRNA or lncRNA in prostate cancer and diffuse large B cell lymphoma [10, 11]. starBase predicted that RNASEH1-AS1 and BUD13 had mutual binding sequences, indicating BUD13 might be involved in CRC development as an RBP for RNASEH1-AS1. In addition, we found there were potential binding sequences



between BUD13 and Annexin A2 (ANXA2). ANXA2 was identified as an oncogene in various tumors including CRC by massive research [12, 13]. Therefore, we speculated that RNASEH1-AS1 might recruit BUD13 to stabilize ANXA2 mRNA and elevate ANXA2 expression, thus promoting the progression of CRC.

It is well-known that Histone H3 on lysine 27 acetylation (H3K27ac) is mainly enriched in enhancer and promoter regions of genes and is closely related to gene activation [14]. Growing studies have reported that the expression of lncRNAs such as lncRNA KTN1-AS1 and lncRNA PAXIP1-AS1 were activated and elevated by H3K27ac induction, further aggravating tumor progression [14, 15]. Encouragingly, through searching the UCSC database, H3K27ac enrichment was found in the RNASEH1-AS1 promoter region. Hence, the abnormally high RNASEH1-AS1 expression in CRC might be implicated in H3K27ac induction.

Depending on the above evidence, we reasonably conjectured that H3K27ac-induced RNASEH1-AS1 stabilizes ANXA2 mRNA and elevates ANXA2 expression, thereby accelerating CRC progression by promoting CRC cell viability, proliferation, migration, and invasion. Our findings might provide new molecular targets for CRC therapy in the future.

Patients and methods

Patients and tissue samples. The samples including cancerous tissues and para-cancerous tissues were collected from patients (50 cases) who were diagnosed with CRC and did not receive chemotherapy or radiotherapy in Zhongshan Hospital (Xiamen), Fudan University; Xiamen Clinical Research Center for Cancer Therapy. The samples were preserved in the refrigerator at -80°C . This study was approved by the Ethics Committee of Zhongshan Hospital (Xiamen), Fudan University; Xiamen Clinical Research Center for Cancer Therapy, and informed consent was obtained.

Cell culture and treatment. The normal colonic epithelial cell line (NCM460 cells) was purchased from iCell (China) and CRC cells (HCT116, SW48, DLD-1, SW620, and SW480) were obtained from ATCC (USA). All cell lines were identified by STR and were free of mycoplasma contamination. NCM460 and CRC cells were cultured in RPMI and the remaining cells were cultured in Dulbecco's modified Eagle's medium (DMEM, Thermo Fisher Scientific, USA) under the condition of 5% CO_2 and 37°C . It needs to be mentioned that the medium was supplemented with 10% FBS (Thermo Fisher Scientific) and 1% antibiotics (Beyotime, China).

20 μM C646 (an inhibitor of histone acetyltransferase, Sigma-Aldrich, USA) was added to SW48 and SW480 cells for 24 h and then for the following experiments.

Cell transfection. The short hairpin RNA targeting CBP (sh-CBP#1, sh-CBP#2) or BUD13 (sh-BUD13#1, sh-BUD13#2), and sh-NC as control were obtained from

GenePharma (China). RNASEH1-AS1 overexpression vector (OE-RNASEH1-AS1) was also bought from GenePharma (China). SW48 and SW480 cells were seeded into 6-well plates and incubated overnight. Then, cells were transfected with the above plasmids for 48 h using Lipofectamine™ 3000 (Invitrogen, USA) following the instructions. Lentivirus carrying sh-RNASEH1-AS1 or overexpression vector of ANXA2 (OE-ANXA2) were also bought from GenePharma (China). Moderate viral supernatant was added to SW48 and SW480 cells. After 24 h infection, the medium containing the virus was replaced with a fresh medium to continuously culture cells.

RT-qPCR. Total RNA was acquired from samples including clinical tissues, cells, and animal tissues using TRIzol reagent (Beyotime). After cDNA synthesis was performed using Script Reverse Transcription Reagent Kit (TaKaRa, Japan), SYBR Premix Ex Taq II Kit (TaKaRa) was used for the qPCR process. The real-time fluorescent quantitative PCR test was run for 40 cycles using the following reaction conditions: 10 min of pre-denaturation at 95°C , 10 s denaturation at 95°C , 20 s annealing at 60°C , and 34 s extension at 72°C . The primer sequences were as follows: RNASEH1-AS1 (F): 5'-GCGGATCTACAGTAAGGGCTGT-3'; RNASEH1-AS1 (R): 5'-CGCCCTCCTTTGTGCTTATTC-3'; CBP (F): 5'-CAACCCCAAAAGAGCCAAACT-3'; CBP (R): 5'-CCTCGTAGAAGCTCCGACAGT-3'; BUD13 (F): 5'-TGCGGATTGTGGATGATGATGTGAG-3'; BUD13 (R): 5'-GCCTCCATCTGCTTTACCTCTTCTG-3'; ANXA2 (F): 5'-TCTACTGTTTACGAAATCCTGTG-3'; ANXA2 (R): 5'-AGTATAGGCTTTGACAGACCCAT-3'; GAPDH (F): 5'-GGTGTGAACCATGAGAAGTATGA-3'; GAPDH (R): 5'-GAGTCCTTCCACGATACCAAAG-3'. All data were calculated by using the $2^{-\Delta\Delta\text{Ct}}$ formula. GAPDH served as a reference gene.

Cell count kit-8 (CCK-8) assay. SW48 and SW480 cells with indicated transfections were implanted onto 96-well plates at the density of 1×10^4 cells/well and cultured for 24 h. 10 μl CCK-8 solution from a commercial kit (Beyotime) was added into each well. After 2 h incubation, the absorbance was detected at 450 nm in wavelength by a spectrophotometer (Bio-Rad, Hercules, USA).

Clone formation assay. SW48 and SW480 cells with indicated transfections were seeded on 6-well plates (500 cells/well) and were incubated. 2 weeks later, methanol and 0.1% crystalized violet (Sigma-Aldrich) were used to fix and stain cells, respectively. An inverted microscope (Olympus, Japan) was employed to observe the cloned cells.

Wound healing assay. SW48 and SW480 cells with indicated transfections were implanted on 6-well plates (5×10^3 /well) with cellular monolayers. Once the cells were attached to the wall, cells were scraped with a micropipette tip. After washing with PBS, cells were continually cultured for 48 h. The scratched widths were recorded at 0 and 24 h.

Transwell assay. A 24-well Transwell insert system (Corning, USA) was used to examine the invading ability

of SW48 and SW480 cells with indicated transfections. The top Transwell chamber was covered with Matrigel (Becton Dickinson Biosciences, USA). SW48 and SW480 cells (5×10^3) with indicated transfections were seeded onto the upper chamber containing serum-free DMEM and into the lower chamber was added with DMEM supplemented with 10% FBS. After 24 h, the invaded cells on the below side of the chamber were fixed with 95% alcohol. 1% crystal violet (Sigma-Aldrich) stained the invaded cells. An inverted microscope was employed to observe invaded cells.

Chromatin immunoprecipitation (ChIP) assay. SW48 and SW480 cells were collected and then 1% formaldehyde was added to cross-link the DNA and protein in the cells at room temperature for 10 min. After cross-linking, chromatin was sonicated to acquire approximately 200–1000 bp fragments. The cells were centrifuged at $13,000 \times$ at 4°C . The fragments in cell supernatant were incubated with the primary antibody H3K27ac (ab4729, Abcam, UK) or CBP (PA5-27369, Thermo Fisher Scientific) or IgG (ab172730, Abcam) at 4°C overnight. The Protein Agarose/Sepharose precipitated endogenous DNA-protein complexes. After centrifugation, the supernatant was discarded, and the precipitation complex was washed. The immunoprecipitated DNA was analyzed using PCR.

Western blot. The total protein was extracted from samples including cells and animal tissues using RIPA buffer (Beyotime). After quantifying the protein concentration using a BCA protein kit (Beyotime), the same amount of protein (30 μg) was separated by SDS-PAGE and then transferred onto the PVDF membrane. After blocking with 5% BSA for 1 h, the PVDF membrane was incubated with primary antibodies including BUD13 (PA5-58351, 0.1 $\mu\text{g}/\text{ml}$, Thermo Fisher Scientific), ANXA2 (MA5-32689, 1:1000, Thermo Fisher Scientific), β -catenin (ab223075, 1 $\mu\text{g}/\text{ml}$, Abcam), c-Myc (13-2500, 0.8 $\mu\text{g}/\text{ml}$, Thermo Fisher Scientific), cyclin D1 (ab16663, 1:100, Abcam), and GAPDH (ab9485, 1:5000, Abcam) overnight at 4°C . Subsequently, the HRP-conjugated secondary antibody for 1 h was applied to the PVDF membrane. ECL chemiluminescent reagent (Beyotime) and Odyssey Clx Imaging System (Licor Biosciences, USA) were employed to detect protein bands. The densitometry analysis was estimated by ImageJ.

Nucleoplasmic separation. According to the manual, a PARIS™ kit (AM1921, Ambion, USA) separated nuclear and cytoplasmic RNA in SW48 and SW480 cells. GAPDH and U6 served as cytoplasmic control and nuclear control, respectively. RNA-qPCR was applied to detect the levels of RNASEH1-AS1 in the cytoplasm and nucleus.

Fluorescence in situ hybridization (FISH). The expression and location of RNASEH1-AS1 in CRC cells were measured using the FISH assay. A Ribo™ Fluorescent in situ Hybridization Kit (C10910, Ribobio, China) was applied for FISH assay. Briefly, CRC cells were grown on coverslips and fixed for 10 min in 4% formaldehyde at room temperature. Then the cells were rehydrated, digested, and refixed in

4% paraformaldehyde. After that, the cells were prehybridized with a hybridization solution and incubated with an RNASEH1-AS1 probe (GenePharma). Hoechst was used to stain cell nuclei. An inverted microscope (Leica, Germany) was used for the observation of fluorescence.

RNA immunoprecipitation (RIP). A Magna RIP RNA-Binding Protein Immunoprecipitation Kit (Millipore, USA) was applied to conduct the RIP assay. SW48 and SW480 cells (2×10^6 cells/ml) were harvested. RIP Lysis Buffer with protease inhibitor cocktail and RNase inhibitor was applied to lyse harvested cells. After centrifugation, the supernatant was achieved. Part of the supernatant was utilized as an input and a part was incubated with an antibody for co-precipitation. Anti-BUD13 (Thermo Fisher Scientific) or anti-IgG (Thermo Fisher Scientific) were used to incubate cell lysis buffer. After that, the lysates were supplemented with beads containing Proteinase K, and RNA was isolated with TRIzol for immunoprecipitation. RNA enrichment was examined using RT-qPCR.

RNA pull-down assay. The biotin-labeled RNASEH1-AS1 or ANXA2 were provided by Sangon (China) and transfected into SW48 and SW480 cells. The cells were incubated with the streptavidin-coated magnetic beads to construct the probe-covered beads. Then, the bound RNAs were separated from the biotin-coupled RNA complexes and BUD13 enriched by biotin-labeled-RNASEH1-AS1 or ANXA2 was examined using western blot.

Actinomycin D treatment. After transfection with sh-RNASEH1-AS1 or sh-BUD13, SW48 and SW480 cells were treated with 5 mg/ml actinomycin D for 3, 6, 9, or 12 h, respectively. Of note, actinomycin D was used to stop mRNA transcription. ANXA2 mRNA levels were examined by RT-qPCR.

Tumor formation in nude mice. Animal experiments were approved by the ethics committee of Zhongshan Hospital (Xiamen), Fudan University; Xiamen Clinical Research Center for Cancer Therapy. 20 male BALB/c nude mice (4–5 weeks old) were randomly divided into four groups, including Control, sh-NC+OE-NC, sh-RNASEH1-AS1+OE-NC, and sh-RNASEH1-AS1+OE-ANXA2, $n=5/\text{group}$. Lentiviruses carrying sh-RNASEH1-AS1 or sh-RNASEH1-AS1 combined OE-ANXA2 were used to infect SW48 cells. Afterward, subcutaneous injection of SW48 cells generated tumor formation in nude mice. The tumor volume was evaluated every three days for 5 consecutive weeks. After 25 days, mice were sacrificed to remove tumor tissue for subsequent experiments. Animal experiments were approved by the ethics committee of Zhongshan Hospital (Xiamen), Fudan University; Xiamen Clinical Research Center for Cancer Therapy.

Immunohistochemistry (IHC). Tumors from mice were embedded using 4% paraformaldehyde and paraffin. After repairing the antigen, the sections were blocked with 1% BSA and incubated with antibody against Ki-67 (Abcam). HRP-labelled antibody treated the sections. The images were

captured by a Nikon digital camera system combined with an Olympus microscope.

Statistical analysis. All data are presented as means \pm standard deviation (SD). GraphPad Prism 6 was used to analyze all data. Student's t-test and one-way analysis of variance (ANOVA) followed by Tukey test were conducted for comparison of groups. Kaplan-Meier survival analysis was used to generate survival curves and the log-rank test was used to analyze data. A p-value <0.05 was regarded as a statistically significant difference.

Results

RNASEH1-AS1 expression was upregulated in CRC clinical tissues and CRC cells. From the starBase website, RNASEH1-AS1 expression was predicted to be higher in CRC tissues compared to that in para-carcinoma tissues (Figure 1A). In addition, we used RT-qPCR and confirmed that RNASEH1-AS1 expression was higher in clinical tissues from patients with CRC than in matched para-carcinoma tissues (Figure 1B). RNASEH1-AS1 expression in tumor stage III/IV was evidently elevated in relative to stage I/II (Figure 1C). Furthermore, we observed that high expression of RNASEH1-AS1 was associated with poor prognosis in CRC patients (Figure 1D). In several CRC cell lines including HCT116, SW48, DLD-1, SW620, and SW480 cells, RNASEH1-AS1 expression was notably enhanced when compared to NCM460 cells (a normal colonic epithelial cell

line) (Figure 1E). Due to the highest RNASEH1-AS1 expression in SW48 and SW480 cells, these two cells were applied to the following experiments. Altogether, RNASEH1-AS1 might be implicated in CRC progression.

RNASEH1-AS1 knockdown suppressed CRC cell growth, migration, and invasion. To excavate functions of RNASEH1-AS1 on CRC cells, RNASEH1-AS1 expression was silenced in SW48 and SW480 cells using sh-RNASEH1-AS1#1 or #2 transfection. RT-qPCR validated that sh-RNASEH1-AS1#1 or #2 transfection successfully resulted in decreased RNASEH1-AS1 expression in CRC cells, especially in sh-RNASEH1-AS1#1-transfected CRC cells (Figure 2A). Then, a series of experiments were conducted. CCK-8 revealed that cell viability was observably inhibited by RNASEH1-AS1 knockdown (Figure 2B). Clone formation assays confirmed that RNASEH1-AS1 knockdown effectively restrained CRC cell proliferation (Figure 2C). Additionally, the ability of CRC cell migration was apparently attenuated by RNASEH1-AS1 knockdown (Figure 2D). Similarly, cell invasion was suppressed in SW48 and SW480 cells when RNASEH1-AS1 was silenced (Figure 2E). To sum up, RNASEH1-AS1 downregulation could be against CRC progression by inhibiting cell growth, invasion, and migration.

H3K27ac induced RNASEH1-AS1 expression. As previously documented, abnormal expression of lncRNA could be influenced by histone acetylation-mediated transcriptional activation [16]. Hence, we employed the UCSC website to

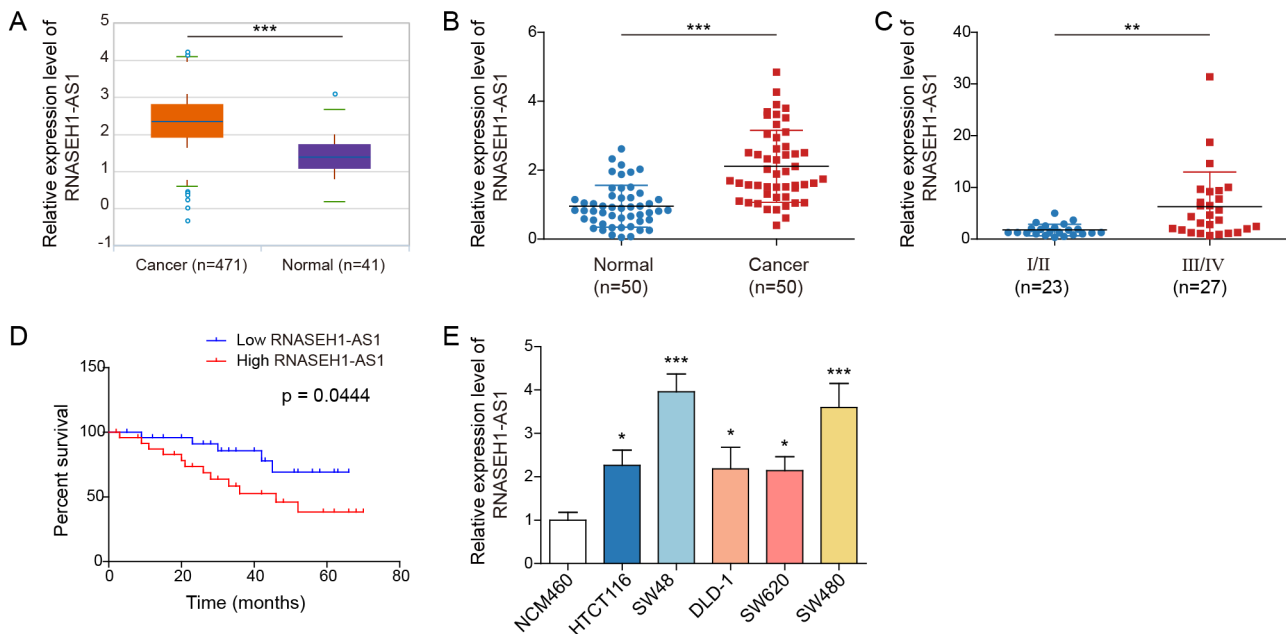


Figure 1. RNASEH1-AS1 expression was upregulated in CRC clinical tissues and CRC cells. A) RNASEH1-AS1 expression was predicted by the starBase database (<http://starbase.sysu.edu.cn>) in CRC. B) RNASEH1-AS1 expression was measured using RT-qPCR in CRC clinical tissues. C) RT-qPCR was used to detect the level of RNASEH1-AS1 in tumor tissues of patients at different clinical stages. D) Kaplan-Meier survival analysis was applied to analyze the relationship between the RNASEH1-AS1 level and survival of CRC patients. E) RNASEH1-AS1 expression was measured using RT-qPCR in NCM460 cells and CRC cells. * $p<0.05$, ** $p<0.01$, *** $p<0.001$

explore how RNASEH1-AS1 was upregulated in CRC. The results predicted that H3K27ac enrichment was predicted in the RNASEH1-AS1 promoter region (Figure 3A). ChIP assay further confirmed that the RNASEH1-AS1 promoter region

was enriched with the H3K27ac antibody in SW48 and SW480 cells (Figure 3B). Noticeably, the enrichment level in SW48 and SW480 cells was apparently higher than that in NCM460 cells (Figure 3B). Intriguingly, when SW48 and

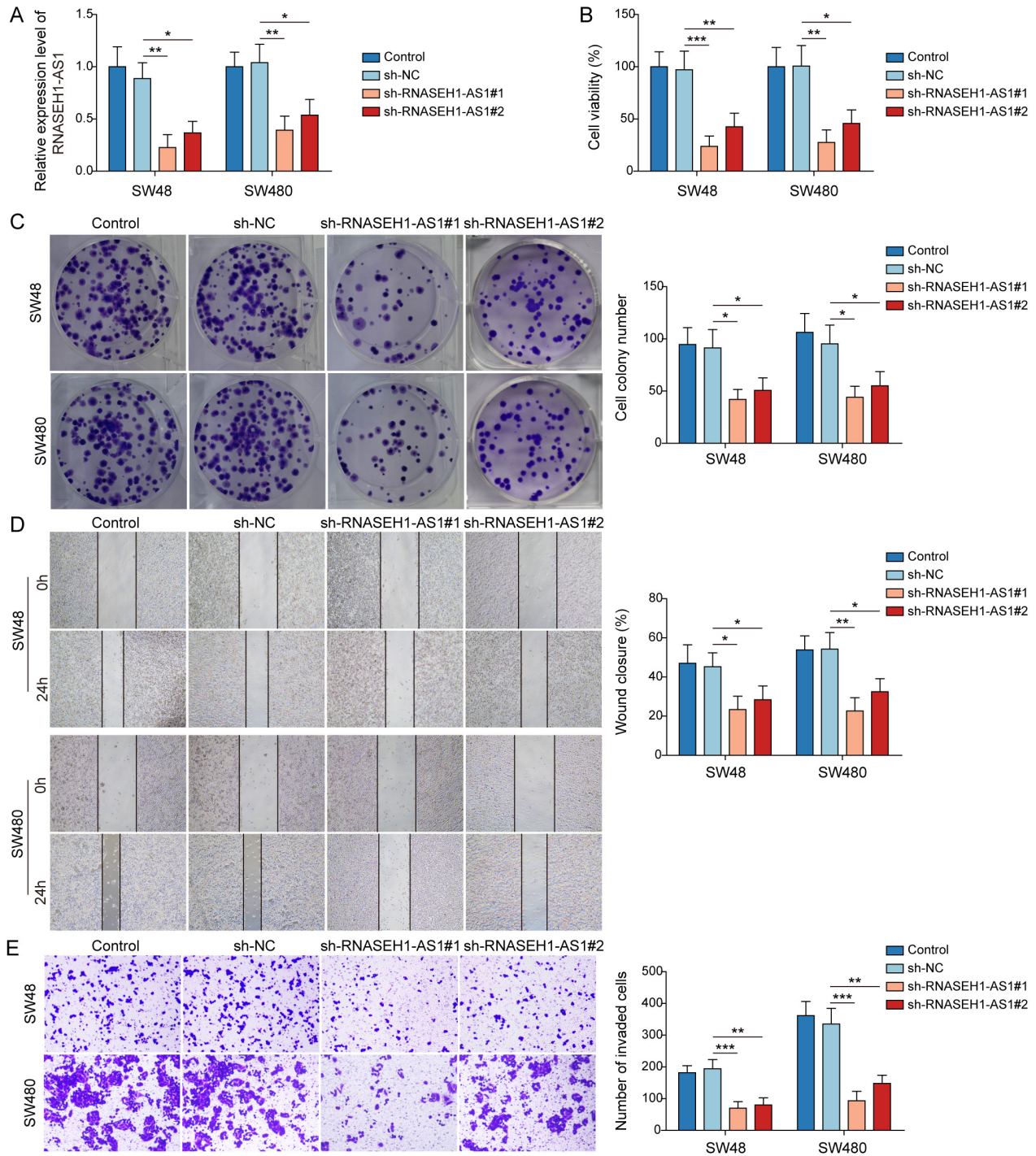


Figure 2. RNASEH1-AS1 knockdown suppressed CRC cell growth, migration, and invasion. RNASEH1-AS1 was silenced in SW48 and SW480 cells using sh-RNASEH1-AS1#1 or #2 transfection. A) The efficiency of RNASEH1-AS1 knockdown was evaluated by RT-qPCR. B) CCK-8 assay evaluated cell viability. C) Clone formation measured cell proliferation. D) Wound healing assay detected cell migration. E) Transwell assay determined cell invasion. * $p < 0.05$, ** $p < 0.01$, *** $p < 0.001$

SW480 cells were treated with an inhibitor of histone acetyltransferase C646, RNASEH1-AS1 expression was found to be observably downregulated (Figure 3C). The above results validated that RNASEH1-AS1 expression in CRC cells was regulated by H3K27ac. Subsequently, we probed how H3K27ac in the RNASEH1-AS1 promoter was regulated. It was reported that CREB binding protein (CBP) was a vital enzyme to be implicated in chromatin acetylation [17]. RT-qPCR assay displayed that CBP expression in CRC cells was notably elevated (Figure 3D). CBP antibody could enrich the RNASEH1-AS1 promoter, which was determined by ChIP (Figure 3E). Then, CBP expression was dramatically knocked down in SW48 and SW480 cells by sh-CBP#1 and sh-CBP#2 (Figure 3F). Concomitantly, RNASEH1-AS1 expression and anti-H3K27ac antibody-mediated RNASEH1-AS1 promoter enrichment were suppressed by CBP knockdown in SW48

and SW480 cells (Figures 3G, 3H). Altogether, our results indicated that higher RNASEH1-AS1 expression in CRC cells was regulated by CBP-mediated H3K27ac.

RNASEH1-AS1 bound to BUD13 in CRC cells. As predicted by the starBase database, RNASEH1-AS1 might bind to a wide variety of RBPs. Herein, we selected 6 RBPs of interest for detection (Supplementary Figure S1A), which have been widely reported to play a role in regulating cancer progression as RBPs by binding with other non-coding RNAs. Through RIP detection, we found that among these RBPs, only BUD13 had a binding relationship with RNASEH1-AS1 (Supplementary Figure S1B). BUD13 was an RBP that could interact with lncRNA [10]. The mRNA and protein expression of BUD13 was enhanced in SW48 and SW480 cells compared to that in NCM460 cells (Figures 4A, 4B). Nucleoplasmic separation and FISH determined that RNASEH1-

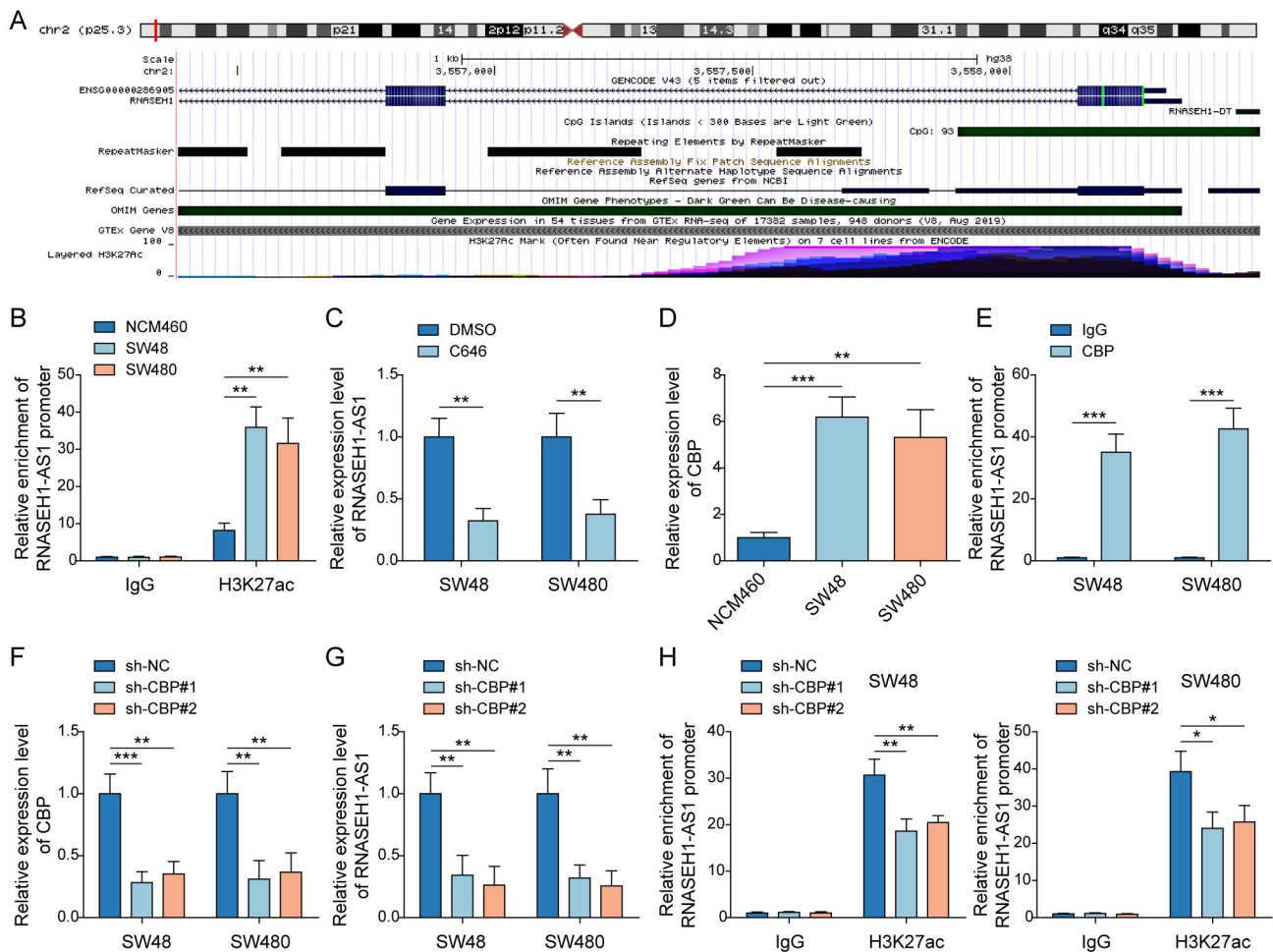


Figure 3. H3K27ac induced RNASEH1-AS1 expression. A) H3K27ac enrichment in the RNASEH1-AS1 promoter was predicted by the UCSC database (<http://genome.ucsc.edu/>). B) The interaction between H3K27ac and the RNASEH1-AS1 promoter was confirmed by ChIP. C) RNASEH1-AS1 expression was detected using RT-qPCR in C646-treated CRC cells. D) CBP expression was examined using RT-qPCR in NCM460, SW48, and SW480 cells. E) The interaction between CBP and the RNASEH1-AS1 promoter was confirmed by ChIP. F) The efficiency of CBP knockdown was evaluated by RT-qPCR. G) RNASEH1-AS1 expression was detected using RT-qPCR in sh-CBP#1 or sh-CBP#2 transfected CRC cells. H) The interaction between H3K27ac and the RNASEH1-AS1 promoter was validated using ChIP in sh-CBP#1 or sh-CBP#2 transfected CRC cells. * $p < 0.05$, ** $p < 0.01$, *** $p < 0.001$

AS1 was distributed in both the nucleus and cytoplasm and was primarily located in the cytoplasm (Figures 4C, 4D). RNA pull-down assays further verified the bound relationship between RNASEH1-AS1 and BUD13 protein in SW48 and SW480 cells, as RNASEH1-AS1 pulled down the BUD13 antibody (Figure 4E).

RNASEH1-AS1 maintained the stability of ANXA2 mRNA in CRC cells by recruiting BUD13. The results of RIP and RNA pull-down found that BUD13 interacted with ANXA2 in SW48 and SW480 cells (Figures 5A–B). To investigate whether ANXA2 is regulated by BUD13, BUD13 expression in CRC cells was silenced by sh-BUD13#1 or #2 transfection (Figure 5C). Actinomycin D, an RNA synthesis inhibitor, was applied to treat CRC cells and detected ANXA2 mRNA levels. We found that BUD13 silencing significantly increased the degradation of ANXA2 mRNA (Figure 5D). Furthermore, ANXA2 mRNA and protein levels in CRC cells were significantly declined by the BUD13 silencing (Figures 5E, 5F). RIP assay showed that sh-RNASEH1-AS1#1 significantly decreased the binding of BUD13 to ANXA2 (Figure 5G). In addition, the stability of ANXA2 mRNA was

attenuated by RNASEH1-AS1 knockdown (Figure 5H). As expected, ANXA2 expressions at mRNA and protein level were reduced by RNASEH1-AS1 knockdown (Figures 5I, 5J). To detect whether RNASEH1-AS1 regulates ANXA2 via BUD13, CRC cells were transfected with OE-RNASEH1-AS1 or together with sh-BUD13. Figure 5K displays that RNASEH1-AS1 expression was successfully elevated in CRC cells using OE-RNASEH1-AS1 transfection. Furthermore, we observed that the overexpression of RNASEH1-AS1 significantly upregulated the ANXA2 level. However, BUD13 silencing reversed the promoting effect of RNASEH1-AS1 upregulation on the ANXA2 mRNA level (Figure 5L). These results revealed that RNASEH1-AS1 promoted ANXA2 mRNA stability in CRC cells by recruiting BUD13.

RNASEH1-AS1 knockdown impaired CRC cell growth, migration, and invasion by suppressing the ANXA2/Wnt/ β -catenin axis. We then examined whether RNASEH1-AS1 affected CRC tumor phenotypes by regulating ANXA2. ANXA2 expression was found to be upregulated in SW48 and SW480 cells relative to that in NCM460 cells (Figures 6A, 6B). OE-ANXA2 transfected into CRC cells led to a higher

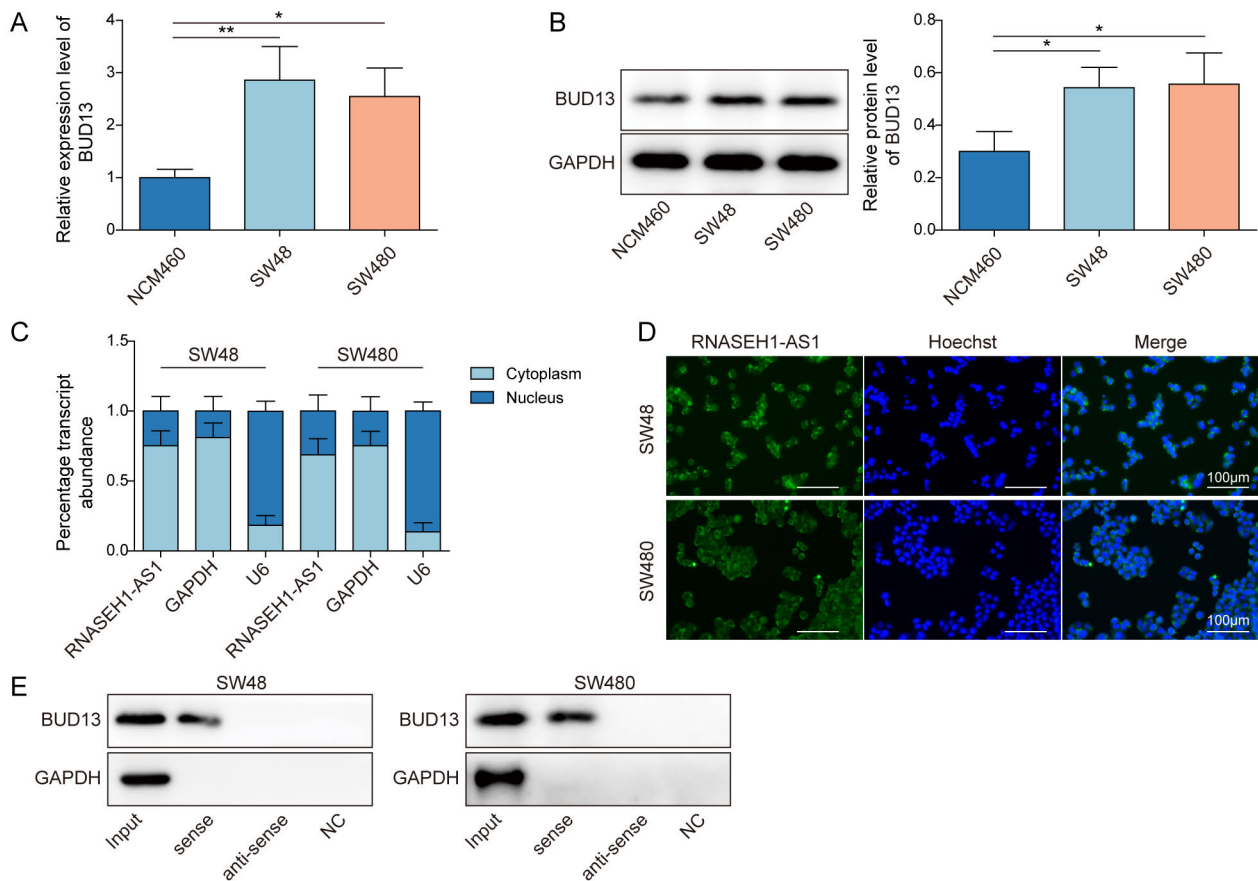


Figure 4. RNASEH1-AS1 bound to BUD13 in CRC cells. **A, B)** The mRNA and protein levels of BUD13 were examined in NCM460, SW48, and SW480 cells using RT-qPCR and western blot, respectively. **C, D)** The location of RNASEH1-AS1 in CRC cells was detected using nucleoplasmic separation and FISH. **E)** The interaction between RNASEH1-AS1 and BUD13 was confirmed by RNA-pull down assay. * $p < 0.05$, ** $p < 0.01$, *** $p < 0.001$

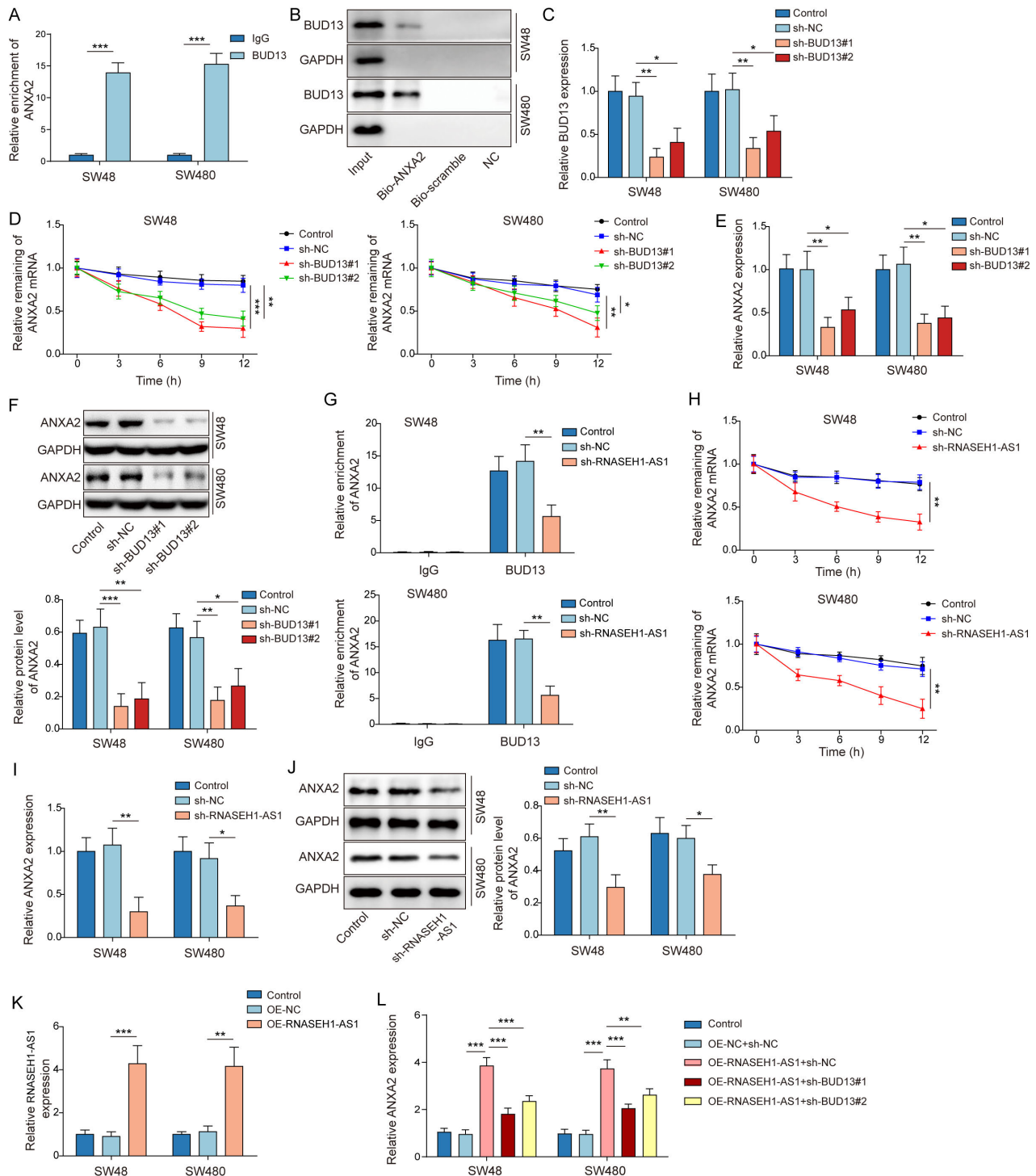


Figure 5. RNASEH1-AS1 maintained the stability of ANXA2 mRNA in CRC cells by recruiting BUD13. **A, B)** The interaction between BUD13 and ANXA2 was verified by RIP and RNA pull-down. **C)** The efficiency of BUD13 knockdown was evaluated by RT-qPCR. **D)** ANXA2 mRNA levels in sh-BUD13#1 or #2 transfected CRC cells upon actinomycin D were examined using RT-qPCR. **E, F)** The mRNA and protein levels of ANXA2 were examined in sh-BUD13#1 or #2 transfected CRC cells using RT-qPCR and western blot. **G)** The interaction between BUD13 and ANXA2 in sh-RNASEH1-AS1#1 transfected CRC cell was validated using RIP. **H)** ANXA2 mRNA levels in sh-RNASEH1-AS1 transfected CRC cells upon actinomycin D were examined using RT-qPCR. **I, J)** The mRNA and protein levels of ANXA2 were examined in sh-RNASEH1-AS1#1 transfected CRC cell using RT-qPCR and western blot. **K)** RNASEH1-AS1 expression was detected in CRC cells transfected with OE-NC or OE-RNASEH1-AS1 using RT-qPCR. **L)** The mRNA level of ANXA2 in CRC cells with OE-RNASEH1-AS1 or together with sh-BUD13 transfection was detected using RT-qPCR. * $p < 0.05$, ** $p < 0.01$, *** $p < 0.001$

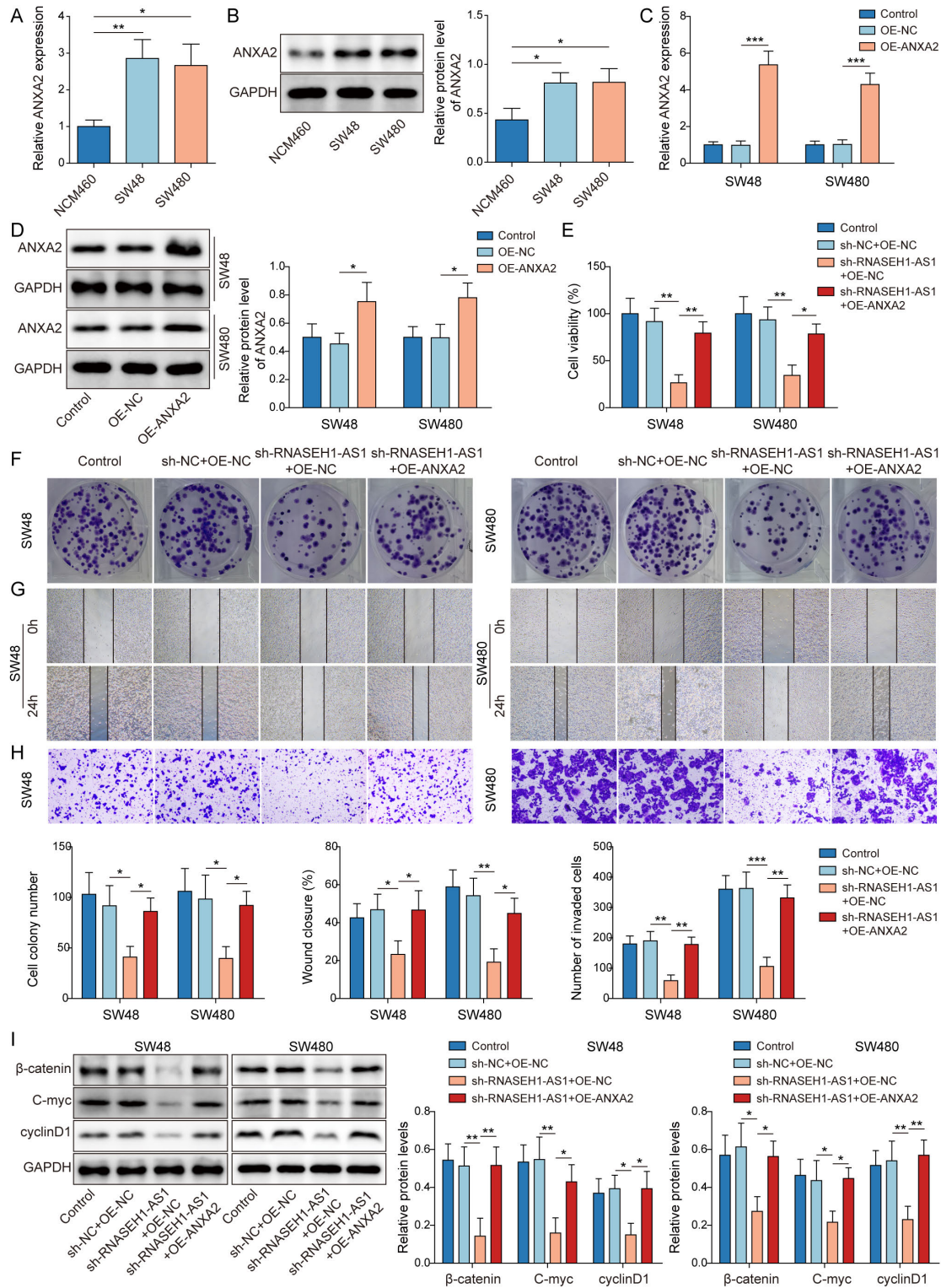


Figure 6. RNASEH1-AS1 knockdown impaired CRC cell growth, migration, and invasion by suppressing the ANXA2/Wnt/ β -catenin axis. **A, B)** The mRNA and protein levels of ANXA2 were examined in NCM460, SW48, and SW480 cells using RT-qPCR and western blot. **C, D)** The efficiency of ANXA2 overexpression was evaluated by RT-qPCR and western blot. SW48 and SW480 cells were transfected with sh-RNASEH1-AS1#1 or in combination with OE-ANXA2. **E)** CCK-8 assay evaluated cell viability. **F)** Clone formation measured cell proliferation. **G)** Wound healing assay detected cell migration. **H)** Transwell assay determined cell invasion. **I)** Wnt/ β -catenin pathway-related proteins including β -catenin, c-Myc, and cyclin D1 were determined by western blot. * $p < 0.05$, ** $p < 0.01$, *** $p < 0.001$

expression of ANXA2 in CRC cells (Figures 6C, 6D). To clarify whether ANXA2 is involved in RNASEH1-AS1 knockdown-mediated inhibition of malignant phenotypes in CRC cells, OE-ANXA2 was transfected in sh-RNASEH1-AS1-transfected CRC cells. We observed that ANXA2 overexpression abolished RNASEH1-AS1 silencing-mediated suppressing effect on CRC cell viability (Figure 6E). Clone formation assay revealed that inhibition of CRC cell proliferation caused by RNASEH1-AS1 silencing was attenuated by ANXA2 overexpression (Figure 6F). Similarly, RNASEH1-AS1 knockdown-mediated inhibitory influences on CRC cell invasion and migration were impaired by ANXA2 overexpression (Figures 6G, 6H). Additionally, the protein levels of Wnt/ β -catenin signaling molecules (β -catenin, c-Myc, and cyclin D1) were inhibited by RNASEH1-AS1 knockdown, which was reversed by ANXA2 overexpression (Figure 6I), indicating RNASEH1-AS1 knockdown suppressed Wnt/ β -

catenin pathway by reducing ANXA2 expression. Therefore, we summarized that RNASEH1-AS1 knockdown inactivated the Wnt/ β -catenin pathway to restrain CRC progression by declining the ANXA2 expression.

RNASEH1-AS1 promoted tumorigenesis in mice by regulating the ANXA2/Wnt/ β -catenin axis. Then, we established xenograft models bearing sh-RNASEH1-AS1 with/without OE-ANXA2-transfected SW48 cells in nude mice to verify the effects of RNASEH1-AS1/ANXA2 axis in CRC cells. As shown in Figures 7A–7C, tumor volume and weight were evidently suppressed in the sh-RNASEH1-AS1 group relative to control and sh-NC+OE-NC groups, however, ANXA2 overexpression reversed sh-RNASEH1-AS1-mediated inhibition of tumor growth. In addition, the IHC assay exhibited that Ki-67 expression was reduced by RNASEH1-AS1 silencing, which was abolished by ANXA2 overexpression (Figure 7D). Expectedly, ANXA2 overexpression

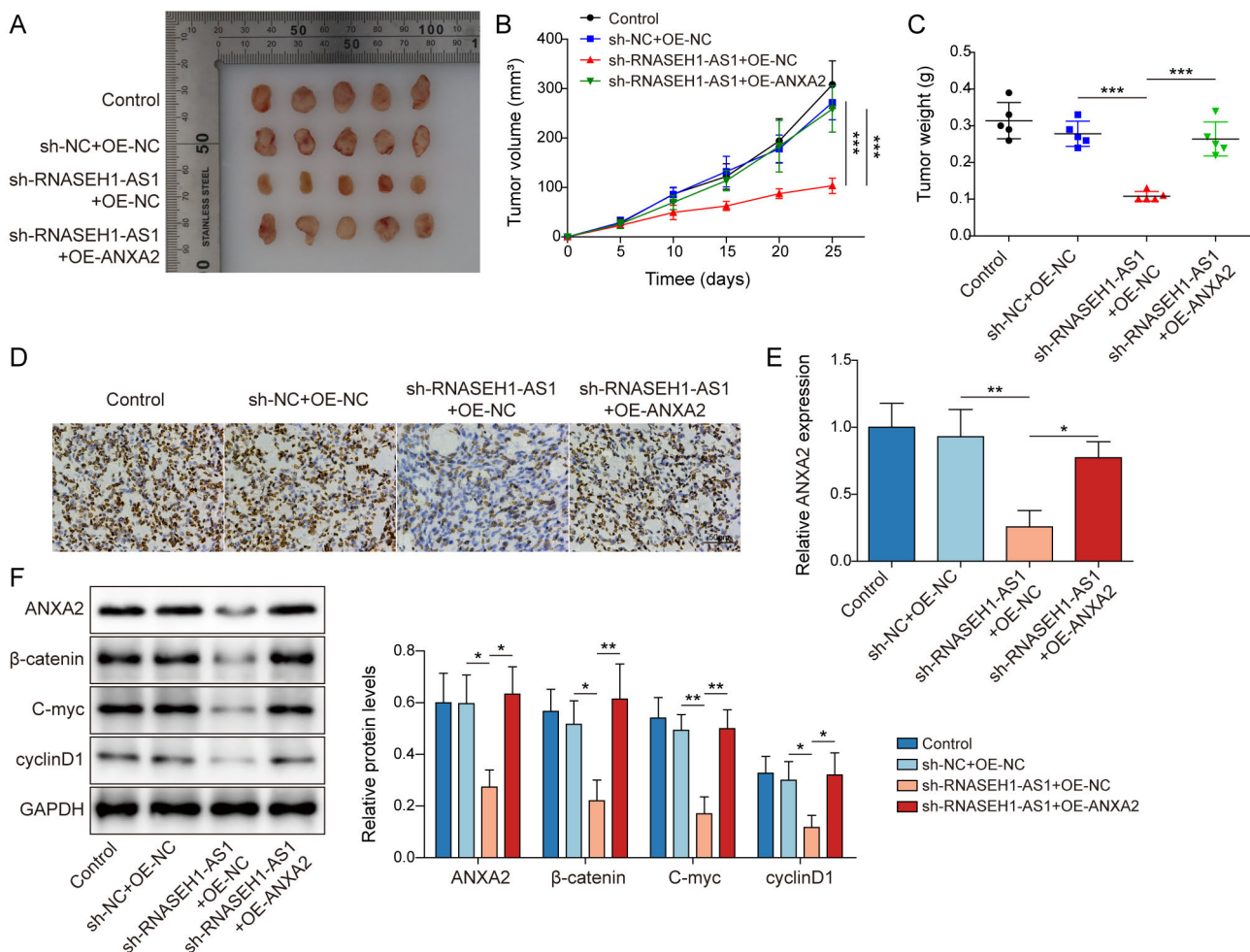


Figure 7. RNASEH1-AS1 promoted tumorigenesis in mice by regulating the ANXA2/Wnt/ β -catenin axis. Nude mice were injected subcutaneously with SW48 cells transfected with sh-RNASEH1-AS1#1 or in combination with OE-ANXA2. A) Tumor images. B) Tumor volume. C) Tumor weight. D) Ki-67 expression was detected using IHC. E) ANXA2 expression was detected using RT-qPCR. F) The protein levels of ANXA2, β -catenin, c-Myc, and cyclin D1 were determined by western blot. * $p < 0.05$, ** $p < 0.01$, *** $p < 0.001$

restored RNASEH1-AS1 silencing-mediated reduction of ANXA2 expression in tumors (Figures 7E, 7F). Downregulation of β -catenin, c-Myc, and cyclin D1 expression caused by RNASEH1-AS1 knockdown was reversed by ANXA2 overexpression (Figure 7F). In summary, RNASEH1-AS1 knockdown suppressed tumor formation in mice by suppressing the ANXA2/Wnt/ β -catenin axis.

Discussion

The early symptoms of CRC are insidious, leading to the fact that most patients are already in the advanced stage at the time of diagnosis, accompanied by tumor cell metastasis, which greatly increases the difficulty of clinical treatment [18]. As growing evidence indicated, it is of great significance to explore the pathogenesis of CRC and find early markers from molecular mechanism [19]. It was reported that lncRNAs play crucial roles in cancers including CRC [20]. In this study, we concentrated on the role of RNASEH1-AS1 in CRC. Our findings revealed that RNASEH1-AS1 induced by H3K27ac could promote ANXA2 mRNA stability by recruiting BUD13, thereby activating the Wnt/ β -catenin axis and facilitating CRC progression.

lncRNAs have been extensively evidenced by numerous studies to be involved in affecting cell growth and metastasis of various cancers [21]. For CRC, lncRNA NALT1 regulated miRNA-574-5p/PEG10 axis to accelerate CRC progression by promoting cell proliferation, migration, and invasion [22]. lncRNA ELFN1-AS1 promoted malignant phenotypes of CRC cells through silencing TPM1 [23]. Furthermore, various lncRNAs were proposed as biomarkers for diagnosis and prognosis in CRC [24]. A review summarized that lncRNA MALAT1 was identified as a diagnostic, predictive, and prognostic biomarker of CRC [25]. Because starBase revealed that RNASEH1-AS1 was highly expressed in CRC, this quickly attracted our attention. Furthermore, published studies until now related to RNASEH1-AS1 are limited to its high expression in NSCLC, and its inhibition could suppress cell growth and metastasis [7]. However, the abundance, functions, and mechanism of RNASEH1-AS1 in CRC are still blank. In this study, we achieved CRC tissues from patients and mice, as well as CRC cells, and we found RNASEH1-AS1 expression was boosted in these experimental subjects, suggesting RNASEH1-AS1 had a great possibility to be engaged in CRC progression. Moreover, RNASEH1-AS1 knockdown effectively suppressed cell growth and invasion in CRC cells as well as tumor formation in mice. Taken together, we first confirmed the driving role of RNASEH1-AS1 on malignant behaviors in CRC.

Mounting evidence focused on H3K27ac in cancers which could activate gene expression to influence cell phenotypes [16]. It was reported that H3K27ac could be mediated by CBP, a histone acetyltransferase, and H3K27ac was associated with higher transcriptional activation, so it can regulate the expression of target genes by regulating the transcriptional

activity of downstream target genes [2]. Some lncRNAs have been documented to be regulated by H3K27ac. For example, H3K27ac enrichment in the PAXIP1-AS1 promoter region resulted in upregulation of PAXIP1-AS1 expression, which promoted cell growth and metastasis in ovarian cancer by regulating the miR-6744-5p/PCBP2 axis [15]. H3K27ac-induced FOXC2-AS1 promoted E2F3 expression, thereby accelerating tongue squamous cell carcinoma [26]. In our study, we found H3K27ac enrichment in the RNASEH1-AS1 promoter by browsing the UCSC database. Simultaneously, the ChIP assay validated the interaction between H3K27ac and the RNASEH1-AS1 promoter. Besides, we found that C646 (an inhibitor of histone acetyltransferase) inhibited the RNASEH1-AS1 expression. Thus, we concluded that the abnormally high expression of RNASEH1-AS1 in CRC was possibly induced by H3K27ac. CBP was recognized as a crucial regulator for histone acetylation as well as gene transcription [17]. In the current study, CBP expression was found to be higher in CRC cells than in NCM460 cells. Moreover, CBP knockdown attenuated RNASEH1-AS1 expression and the interaction between H3K27ac and RNASEH1-AS1. Hence, we firstly determined that RNASEH1-AS1 promoter was labeled by H3K27ac because of interacting with histone acetyltransferase CBP, thus triggering enhancer activation of RNASEH1-AS1 and gene transcription.

Here, we mainly discussed the downstream molecular regulatory mechanisms of RNASEH1-AS1. As described formerly, RBPs play vital roles in the mediation of cancers and the mechanism of lncRNA-RBP axis in cancers was widely investigated [27]. Growing studies indicated that lncRNA recruited RBP to stabilize targeted genes' mRNA and enhanced genes' expression. For example, lncRNA NPSR1-AS1 stabilized NPSR1 mRNA to facilitate thyroid cancer through recruiting ELAVL1 [28]. As previously documented, BUD13 is an RBP that binds to target mRNA to regulate mRNA stability. Chen *et al.* revealed that BUD13 served as an Fbw7 E3 ligase binding partner and regulator by competing with Fbw7 substrates binding to Fbw7 in stabilizing Fbw7 oncogenic substrates, exerting an oncogenic role in CRC [29]. Additionally, BUD13 as an RBP was recruited by lncRNA DBH-AS1 to stabilize FN1 mRNA [10]. BUD13, mediated m6A modification by METTL3, enhanced the stability of CDK12 mRNA and upregulated its expression in glioblastoma cells [30]. CircSERPINA3 could stabilize SERPINA3 mRNA via recruiting BUD13 to affect cell apoptosis, autophagy, and aerobic glycolysis in prostate cancer [11]. Our findings revealed that BUD13 expression was elevated in CRC cells. Besides, the RIP and RNA pull-down test found that BUD13 interacted with RNASEH1-AS1 and ANXA2. ANXA2 belongs to the calcium-mediated phospholipid binding protein family, which was identified as a biomarker for aggressive cancers [31]. Furthermore, previous studies pointed out that ANXA2 promoted CRC progression by affecting malignant behaviors [32]. Consistently, we found that ANXA2 had abnormally high expres-

sion in CRC cells. Of note, ANXA2 overexpression impaired RNASEH1-AS1 knockdown-mediated suppression of malignant phenotypes of CRC cells and tumor formation in mice. Collectively, we evidenced that RNASEH1-AS1 recruited BUD13 to stabilize ANXA2 mRNA and elevated ANXA2 expression, thereby promoting CRC cell proliferation, migration, and invasion.

Accumulating evidence has demonstrated that the Wnt/ β -catenin pathway is engaged in the initiation and progression of numerous cancers, including CRC [33, 34]. As reported previously, lncRNAs could influence CRC progression by activating the Wnt/ β -catenin pathway [35]. For instance, lncRNA NEAT1 activated the Wnt/ β -catenin signaling to promote CRC cell growth by interacting with DDX5 [36]. Here, our findings exhibited RNASEH1-AS1 knockdown inactivated the Wnt/ β -catenin pathway *in vitro* and *in vivo*, suggesting that RNASEH1-AS1 promoting CRC progression was realized through activating the Wnt/ β -catenin pathway. In addition, the positive correlation between ANXA2 and the Wnt/ β -catenin pathway was established in hepatocellular carcinoma and breast cancer [37, 38]. Currently, there are no studies reporting the relationship between ANXA2 and the Wnt/ β -catenin pathway in CRC. In our study, we found ANXA2 overexpression abolished RNASEH1-AS1 knockdown-mediated suppression of the Wnt/ β -catenin pathway *in vitro* and *in vivo*. Therefore, we proposed that RNASEH1-AS1 activated the Wnt/ β -catenin pathway to accelerate CRC progression by elevating ANXA2 expression.

In conclusion, we firstly determined that H3K27ac-induced RNASEH1-AS1 activated Wnt/ β -catenin pathway to accelerate CRC progression by recruiting BUD13 to stabilize ANXA2 mRNA and to elevate ANXA2 expression. Our findings laid the experimental foundation for RNASEH1-AS1 in CRC and might provide molecular therapeutic targets for CRC therapy.

Supplementary information is available in the online version of the paper.

References

- [1] SUNG H, FERLAY J, SIEGEL RL, LAVERSANNE M, SOERJOMATARAM I et al. Global Cancer Statistics 2020: GLOBOCAN Estimates of Incidence and Mortality Worldwide for 36 Cancers in 185 Countries. *CA Cancer J Clin* 2021; 71: 209–249. <https://doi.org/10.3322/caac.21660>
- [2] ANDRE N, SCHMIEGEL W. Chemoradiotherapy for colorectal cancer. *Gut* 2005; 54: 1194–1202. <https://doi.org/10.1136/gut.2004.062745>
- [3] BILLER LH, SCHRAG D. Diagnosis and Treatment of Metastatic Colorectal Cancer: A Review. *JAMA* 2021; 325: 669–685. <https://doi.org/10.1001/jama.2021.0106>
- [4] BRIDGES MC, DAULAGALA AC, KOURTIDIS A. LNCcation: lncRNA localization and function. *J Cell Biol* 2021; 220: e202009045. <https://doi.org/10.1083/jcb.202009045>
- [5] REN C, HAN H, PAN J, CHANG Q, WANG W et al. DLGAP1-AS2 promotes human colorectal cancer progression through trans-activation of Myc. *Mamm Genome* 2022; 33: 672–683. <https://doi.org/10.1007/s00335-022-09963-y>
- [6] YU Z, WANG X, NIU K, SUN L, LI D. LncRNA TM4SF19-AS1 exacerbates cell proliferation, migration, invasion, and EMT in head and neck squamous cell carcinoma via enhancing LAMC1 expression. *Cancer Biol Ther* 2022; 23: 1–9. <https://doi.org/10.1080/15384047.2022.2116923>
- [7] ZHANG C, HUANG J, LOU K, OUYANG H. Long noncoding RNASEH1-AS1 exacerbates the progression of non-small cell lung cancer by acting as a ceRNA to regulate microRNA-516a-5p/FOXK1 and thereby activating the Wnt/ β -catenin signaling pathway. *Cancer Med* 2022; 11: 1589–1604. <https://doi.org/10.1002/cam4.4509>
- [8] FERRÈ F, COLANTONI A, HELMER-CITTERICH M. Revealing protein-lncRNA interaction. *Brief Bioinform* 2016; 17: 106–116. <https://doi.org/10.1093/bib/bbv031>
- [9] PAN L, LI Y, JIN L, LI J, XU A. TRPM2-AS promotes cancer cell proliferation through control of TAF15. *Int J Biochem Cell Biol* 2020; 120: 105683. <https://doi.org/10.1016/j.biocel.2019.105683>
- [10] SONG Y, GAO F, PENG Y, YANG X. Long non-coding RNA DBH-AS1 promotes cancer progression in diffuse large B-cell lymphoma by targeting FN1 via RNA-binding protein BUD13. *Cell Biol Int* 2020; 44: 1331–1340. <https://doi.org/10.1002/cbin.11327>
- [11] XING Z, LI S, LIU Z, ZHANG C, BAI Z. CircSERPINA3 regulates SERPINA3-mediated apoptosis, autophagy and aerobic glycolysis of prostate cancer cells by competitively binding to MiR-653-5p and recruiting BUD13. *J Transl Med* 2021; 19: 492. <https://doi.org/10.1186/s12967-021-03063-2>
- [12] LI Z, YU L, HU B, CHEN L, JI M et al. Advances in cancer treatment: a new therapeutic target, Annexin A2. *J Cancer* 2021; 12: 3587–3596. <https://doi.org/10.7150/jca.55173>
- [13] ZHOU L, LI J, LIAO M, ZHANG Q, YANG M. LncRNA MIR155HG induces M2 macrophage polarization and drug resistance of colorectal cancer cells by regulating ANXA2. *Cancer Immunol Immunother* 2022; 71: 1075–1091. <https://doi.org/10.1007/s00262-021-03055-7>
- [14] XIE X, WEN Q, YANG X, CHEN W, LIU Y et al. H3K27ac-activated lncRNA KTN1-AS1 aggravates tumor progression by miR-505-3p/ZNF326 axis in ovarian cancer. *Ann Transl Med* 2022; 10: 599. <https://doi.org/10.21037/atm-22-443>
- [15] MA Y, ZHENG W. H3K27ac-induced lncRNA PAXIP1-AS1 promotes cell proliferation, migration, EMT and apoptosis in ovarian cancer by targeting miR-6744-5p/PCBP2 axis. *J Ovarian Res* 2021; 14: 76. <https://doi.org/10.1186/s13048-022-01038-5>
- [16] YE P, LV X, AIZEMAITI R, CHENG J, XIA P et al. H3K27ac-activated LINC00519 promotes lung squamous cell carcinoma progression by targeting miR-450b-5p/miR-515-5p/YAP1 axis. *Cell Prolif* 2020; 53: e12797. <https://doi.org/10.1111/cpr.12797>
- [17] BOSE DA, DONAHUE G, REINBERG D, SHIEKHATTAR R, BONASIO R et al. RNA Binding to CBP Stimulates Histone Acetylation and Transcription. *Cell* 2017; 168: 135–149. e22. <https://doi.org/10.1016/j.cell.2016.12.020>

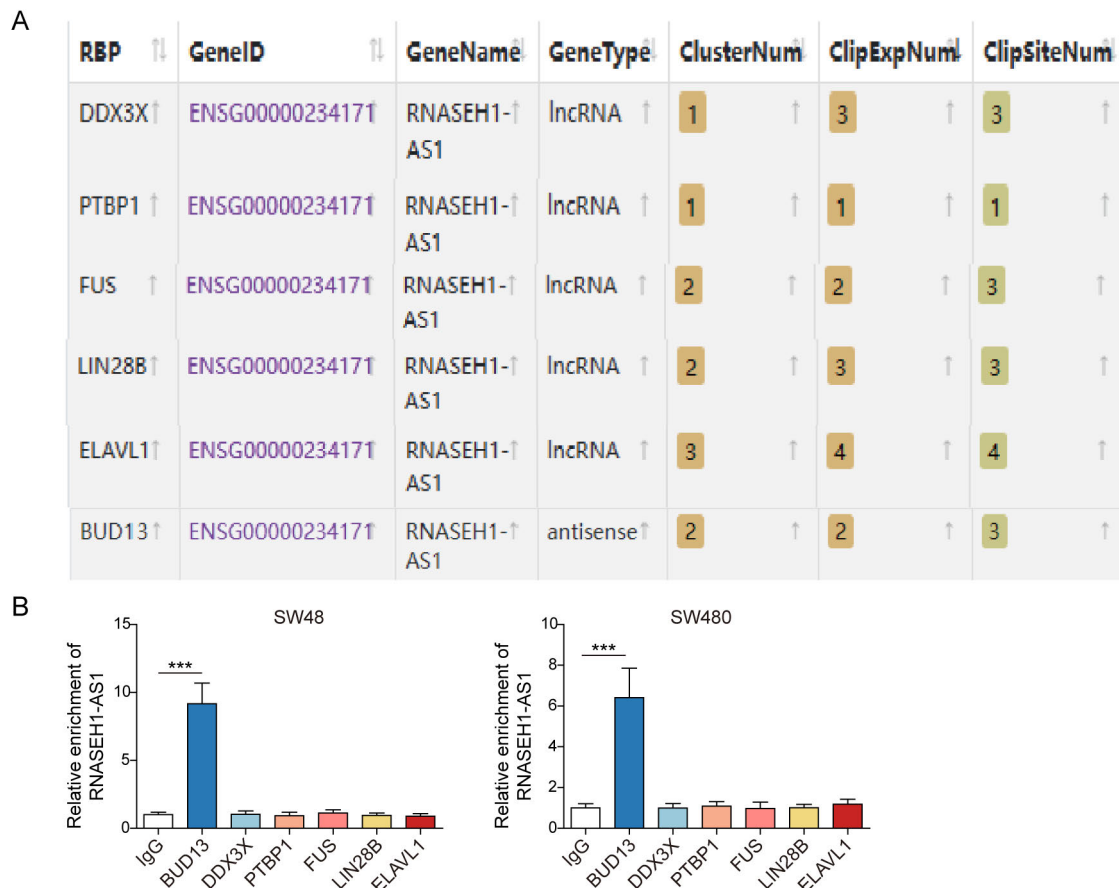
- [18] HAO TB, SHI W, SHEN XJ, QI J, WU XH et al. Circulating cell-free DNA in serum as a biomarker for diagnosis and prognostic prediction of colorectal cancer. *Br J Cancer* 2014; 111: 1482–1489. <https://doi.org/10.1038/bjc.2014.470>
- [19] PIAWAH S, VENOOK AP. Targeted therapy for colorectal cancer metastases: A review of current methods of molecularly targeted therapy and the use of tumor biomarkers in the treatment of metastatic colorectal cancer. *Cancer* 2019; 125: 4139–4147. <https://doi.org/10.1002/cncr.32163>
- [20] WANG Y, LU JH, WU QN, JIN Y, WANG DS et al. LncRNA LINRIS stabilizes IGF2BP2 and promotes the aerobic glycolysis in colorectal cancer. *Mol Cancer* 2019; 18: 174. <https://doi.org/10.1186/s12943-019-1105-0>
- [21] BHAN A, SOLEIMANI M, MANDAL SS. Long Noncoding RNA and Cancer: A New Paradigm. *Cancer Res* 2017; 77: 3965–3981. <https://doi.org/10.1158/0008-5472.CAN-16-2634>
- [22] YE M, ZHAO L, ZHANG L, WU S, LI Z et al. LncRNA NALT1 promotes colorectal cancer progression via targeting PEG10 by sponging microRNA-574-5p. *Cell Death Dis* 2022; 13: 960. <https://doi.org/10.1038/s41419-022-05404-5>
- [23] LI C, HONG S, HU H, LIU T, YAN G et al. MYC-Induced Upregulation of Lncrna ELFN1-AS1 Contributes to Tumor Growth in Colorectal Cancer via Epigenetically Silencing TPM1. *Mol Cancer Res* 2022; 20: 1697–1708. <https://doi.org/10.1158/1541-7786.MCR-22-0009>
- [24] SNYDER M, IRAOLA-GUZMÁN S, SAUS E, GABALDÓN T. Discovery and Validation of Clinically Relevant Long Non-Coding RNAs in Colorectal Cancer. *Cancers (Basel)* 2022; 14: 3866. <https://doi.org/10.3390/cancers14163866>
- [25] CERVENA K, VODENKOVA S, VYMETALKOVA V. MALAT1 in colorectal cancer: Its implication as a diagnostic, prognostic, and predictive biomarker. *Gene* 2022; 843: 146791. <https://doi.org/10.1016/j.gene.2022.146791>
- [26] CHEN C, CHEN Q, WU J, ZOU H. H3K27ac-induced FOXC2-AS1 accelerates tongue squamous cell carcinoma by upregulating E2F3. *J Oral Pathol Med* 2021; 50: 1018–1030. <https://doi.org/10.1111/jop.13232>
- [27] YAO ZT, YANG YM, SUN MM, HE Y, LIAO L et al. New insights into the interplay between long non-coding RNAs and RNA-binding proteins in cancer. *Cancer Commun (Lond)* 2022; 42: 117–140. <https://doi.org/10.1002/cac2.12254>
- [28] NI T, GUO D, TAN L, Z XIAO Z, SHI Y. NPSR1-AS1 activates the MAPK pathway to facilitate thyroid cancer cell malignant behaviors via recruiting ELAVL1 to stabilize NPSR1 mRNA. *Cell Cycle* 2022; 21: 439–449. <https://doi.org/10.1080/15384101.2021.1979773>
- [29] CHEN J, ZHANG X, TAN X, LIU P. Somatic gain-of-function mutations in BUD13 promote oncogenesis by disrupting Fbw7 function. *J Exp Med* 2023; 220: e20222056. <https://doi.org/10.1084/jem.20222056>
- [30] LIU M, RUAN X, LIU X, DONG W, WANG D et al. The mechanism of BUD13 m6A methylation mediated MBNL1-phosphorylation by CDK12 regulating the vasculogenic mimicry in glioblastoma cells. *Cell Death Dis* 2022; 13: 1017. <https://doi.org/10.1038/s41419-022-05426-z>
- [31] SHARMA MC. Annexin A2 (ANX A2): An emerging biomarker and potential therapeutic target for aggressive cancers. *Int J Cancer* 2019; 144: 2074–2081. <https://doi.org/10.1002/ijc.31817>
- [32] MAO L, YUAN W, CAI K, LAI C, HUANG C et al. EphA2-YES1-ANXA2 pathway promotes gastric cancer progression and metastasis. *Oncogene* 2022; 41: 1228–1230. <https://doi.org/10.1038/s41388-021-02163-z>
- [33] LIU J, XIAO Q, XIAO J, NIU C, LI Y et al. Wnt/ β -catenin signalling: function, biological mechanisms, and therapeutic opportunities. *Signal Transduct Target Ther* 2022; 7: 3. <https://doi.org/10.1038/s41392-021-00762-6>
- [34] ZHANG Y, WANG X. Targeting the Wnt/ β -catenin signaling pathway in cancer. *J Hematol Oncol* 2020; 13: 165. <https://doi.org/10.1186/s13045-020-00990-3>
- [35] ZHOU T, WU L, MA N, TANG F, ZONG Z et al. LncRNA PART1 regulates colorectal cancer via targeting miR-150-5p/miR-520h/CTNBN1 and activating Wnt/ β -catenin pathway. *Int J Biochem Cell Biol* 2020; 118: 105637. <https://doi.org/10.1016/j.biocel.2019.105637>
- [36] ZHANG M, WENG W, ZHANG Q, WU Y, NI S et al. The lncRNA NEAT1 activates Wnt/ β -catenin signaling and promotes colorectal cancer progression via interacting with DDX5. *J Hematol Oncol* 2018; 11: 113. <https://doi.org/10.1186/s13045-018-0656-7>
- [37] TANG T, GUO C, XIA T, ZHANG R, ZEN K et al. LncCCAT1 Promotes Breast Cancer Stem Cell Function through Activating WNT/ β -catenin Signaling. *Theranostics* 2019; 9: 7384–7402. <https://doi.org/10.7150/thno.37892>
- [38] YAN X, ZHANG D, WU W, WU S, QIAN J et al. Mesenchymal Stem Cells Promote Hepatocarcinogenesis via lncRNA-MUF Interaction with ANXA2 and miR-34a. *Cancer Res*, 2017. 77(23): p. 6704–6716. <https://doi.org/10.1158/0008-5472.CAN-17-1915>

https://doi.org/10.4149/neo_2023_230612N303

RNASEH1-AS1 induced by H3K27ac stabilizes ANXA2 mRNA to promote the progression of colorectal cancer through recruiting BUD13

Shengwei ZHUANG[‡], Weihong LU[‡], Lianjun SHEN[‡], Zhekun HUANG, Xiuping ZHANG, Yong ZHANG^{*}

Supplementary Information



Supplementary Figure S1. RNASEH1-AS1 interacted with BUD13 in CRC cells. A. The starBase (<http://starbase.sysu.edu.cn>) database predicted the binding of RNASEH1-AS1 with BUD13, DDX3X, PTBP1, FUS, LIN28B, and ELAVL1. B. RIP assay detected the binding relationship between RNASEH1-AS1 and BUD13, DDX3X, PTBP1, FUS, LIN28B, and ELAVL1. *** $p < 0.001$.